



# Comparison between observed and simulated aeolian snow mass fluxes in Adélie Land, East Antarctica

C. Amory<sup>1,2,3,4</sup>, A. Trouvilliez<sup>1,2,3,4,5</sup>, H. Gallée<sup>1,2</sup>, V. Favier<sup>1,2</sup>, F. Naaim-Bouvet<sup>3,4</sup>, C. Genthon<sup>1,2</sup>, C. Agosta<sup>6</sup>, L. Piard<sup>1,2</sup>, and H. Bellot<sup>3,4</sup>

<sup>1</sup>University of Grenoble Alpes, LGGE, 38041 Grenoble, France

<sup>2</sup>CNRS, LGGE, UMR5183, 38401 Grenoble, France

<sup>3</sup>University of Grenoble Alpes, IRSTEA, 38041 Grenoble, France

<sup>4</sup>IRSTEA, UR ETNA, 38402 Saint-Martin d'Hères, France

<sup>5</sup>Cerema-DTECMF, 29280 Plouzané, France

<sup>6</sup>University of Liège, Department of Geography, 4020 Liège, Belgium

Correspondence to: C. Amory (amory@lgge.obs.ujf-grenoble.fr)

Received: 29 September 2014 – Published in The Cryosphere Discuss.: 5 December 2014

Revised: 28 April 2015 – Accepted: 5 June 2015 – Published: 30 July 2015

**Abstract.** Using the original setup described in Gallée et al. (2013), the MAR regional climate model including a coupled snowpack/aeolian snow transport parameterization, was run at a fine spatial (5 km horizontal and 2 m vertical) resolution over 1 summer month in coastal Adélie Land. Different types of feedback were taken into account in MAR including drag partitioning caused by surface roughness elements. Model outputs are compared with observations made at two coastal locations, D17 and D47, situated respectively 10 and 100 km inland. Wind speed was correctly simulated with positive values of the Nash test (0.60 for D17 and 0.37 for D47) but wind velocities above  $10 \text{ m s}^{-1}$  were underestimated at both D17 and D47; at D47, the model consistently underestimated wind velocity by  $2 \text{ m s}^{-1}$ . Aeolian snow transport events were correctly reproduced with the right timing and a good temporal resolution at both locations except when the maximum particle height was less than 1 m. The threshold friction velocity, evaluated only at D17 for a 7-day period without snowfall, was overestimated. The simulated aeolian snow mass fluxes between 0 and 2 m at D47 displayed the same variations but were underestimated compared to the second-generation FlowCapt<sup>TM</sup> values, as was the simulated relative humidity at 2 m above the surface. As a result, MAR underestimated the total aeolian horizontal snow transport for the first 2 m above the ground by a factor of 10 compared to estimations by the second-generation FlowCapt<sup>TM</sup>. The simulation was significantly improved at D47 if a 1-

order decrease in the magnitude of  $z_0$  was accounted for, but agreement with observations was reduced at D17. Our results suggest that  $z_0$  may vary regionally depending on snowpack properties, which are involved in different types of feedback between aeolian transport of snow and  $z_0$ .

## 1 Introduction

Measurements of aeolian snow mass fluxes in Antarctica revealed that a large amount of snow is transported by the wind (Budd, 1966; Wendler, 1989; Mann et al., 2000; Trouvilliez et al., 2014). The aeolian transport of snow is probably a significant component of the surface mass balance distribution over the Antarctic ice sheet. Although estimates have been proposed based on remote sensing data (Das et al., 2013), reliable quantifications of the contribution of aeolian snow transport processes to the Antarctic surface mass balance (ASMB) can only be assessed by modeling. Previous estimates using numerical models suggest that erosion and blowing snow sublimation represent around 10 % of the net ASMB (Déry and Yau, 2002; Lenaerts et al., 2012a). However, these evaluations were made without considering the complex feedback system between snow surface properties, windborne snow particles, and atmospheric conditions. Indeed, aeolian erosion promotes the formation of snow surface structures such as sastrugi, barchans, dunes, and megadunes,

which, in turn, alter the atmospheric dynamics (Frezzotti et al., 2004). Rougher surfaces reduce the wind speed and the resulting wind-driven erosion of snow (Kodama et al., 1985), but increase turbulence in the near-surface airflow, thereby further increasing the aeolian snow mass flux (Frezzotti et al., 2002). Moreover, the presence of airborne snow particles and their subsequent sublimation are both responsible for an increase in air density, which may reduce turbulence in the surface boundary layer and contribute negatively to snow erosion (Bintanja, 2000; Wamser and Lykossov, 1995). On the other hand, the increase in air density strengthens katabatic flows (Gallée, 1998). An overview of the different types of feedback caused by blowing and drifting snow is given in Gallée et al. (2013).

As previously highlighted (Gallée et al., 2001; Lenaerts et al., 2012b), there are few reliable data sets on aeolian snow transport covering a long period with an hourly temporal resolution, making it difficult to evaluate modeling in Antarctica. One-dimensional (1-D) numerical models have been compared with aeolian snow transport rates in ideal cases (Xiao et al., 2000) and with observations (Lenaerts et al., 2010). Regional climate models have been evaluated against surface mass balance estimates derived from stake networks (Gallée et al., 2005; Lenaerts et al., 2012c). The latter is an integrative method that includes all the components of the surface mass balance: precipitation, run-off, surface and windborne snow sublimation, and erosion/deposition of snow. Aeolian snow transport events simulated by regional climate models have been compared with remote sensing techniques (see Palm et al., 2011), and with visual observations at different polar stations (Lenaerts et al., 2012b) or with particle impact sensors (Lenaerts et al., 2012c). Aeolian snow mass flux measurements are even rarer. Lenaerts et al. (2012b) were only able to evaluate their simulations against annual transport rate values estimated at Terra Nova Bay by the first version of an acoustic sensor FlowCapt™ (Scarchilli et al., 2010), which overestimated aeolian snow mass flux (Trouvilliez et al., 2015), and against an extrapolation of optical particle counter sensor measurements performed at Halley (Mann et al., 2000). To improve analyses, model evaluations thus require more detailed and reliable aeolian snow transport measurements in Antarctica.

Here, we present a detailed comparison between outputs of the regional atmospheric model MAR and data collected during an aeolian snow transport observation campaign in Adélie Land, Antarctica (Trouvilliez et al., 2014). We focus on a 1-month period, (January 2011) during which the observers were in the field and could visually confirm the occurrence of meteorological events. MAR was already evaluated over coastal Adélie Land in terms of the occurrence and qualitative intensity of aeolian snow transport events in January 2010 (Gallée et al., 2013). However, model outputs were only compared with a single point of aeolian snow transport measurements using first-generation FlowCapt™ instruments. These sensors are good at detecting aeolian snow

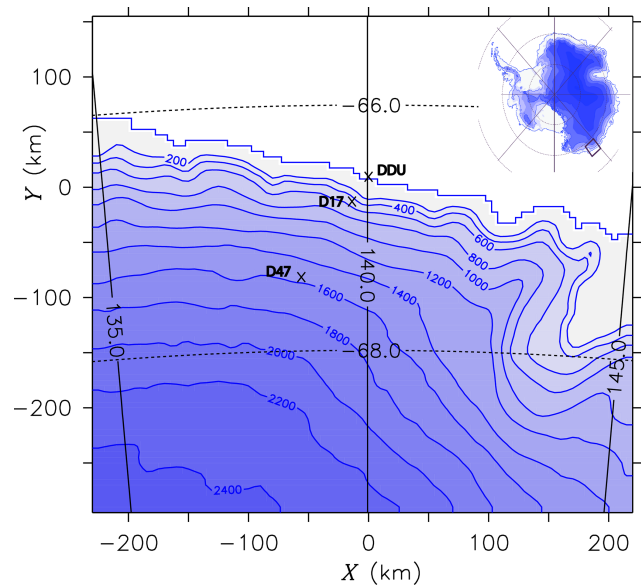


**Figure 1.** Integrative domain of the MAR in Adélie Land, East Antarctica. The crosses mark the location of the French Dumont d'Urville base (DDU) and the two automatic weather and snow stations used in this study (D17 and D47).

transport events but fail to estimate aeolian snow mass fluxes (Cierco et al., 2007; Naaim-Bouvet et al., 2010; Trouvilliez et al., 2015). Second-generation FlowCapt™ instruments were installed at two new locations in February 2010. Unlike its first-generation counterpart, the second-generation sensor is able to provide a lower bound estimate of the aeolian snow mass fluxes (Trouvilliez et al., 2015). It thus allows comparisons not only between the simulated and observed timing of aeolian snow transport events, but also between the simulated and observed aeolian snow mass fluxes, which was previously not the case.

## 2 Field data

Observations were performed in Adélie Land, East Antarctica (Fig. 1), where surface atmospheric conditions are well monitored at the permanent French Dumont d'Urville station (Favier et al., 2011). The coastal region is characterized by frequent strong katabatic winds starting at the break in slope located approximately 250 km inland (Parish and Wendler, 1991; Wendler et al., 1997). These katabatic winds are regularly associated with aeolian snow transport events (Prud'homme and Valtat, 1957; Trouvilliez et al., 2014), making Adélie Land an excellent location for observations of aeolian snow transport. Furthermore, a 40-year accumulation data set is available for Adélie Land and long-term stake measurements are still made along a 150 km stake line (Agosta et al., 2012) and in erosion areas (Genthon et al.,

2007; Favier et al., 2011). These data sets give access to the annual SMB in the area.

Several meteorological campaigns including aeolian snow transport measurements have already been carried out in Adélie Land using mechanical traps (Madigan, 1929; Garcia, 1960; Lorius, 1962) and optical particle counter sensors (Wendler, 1989). However, none of the measurements in Adélie Land or elsewhere in Antarctica fulfill all the requirements of an in-depth evaluation of regional climate models. In 2009, a new aeolian snow transport observation campaign started in Adélie Land, which was specially designed to optimally evaluate models as well as possible, given the prevailing logistical difficulties and limitations (Trouvilliez et al., 2014). In this context, automatic weather stations (AWS) that measure wind speed, wind direction, temperature, relative humidity and snow height at 10 s intervals were installed at three different locations from the coastline to 100 km inland (Trouvilliez et al., 2014). Half-hourly mean values are stored on a Campbell datalogger at each station. The AWS are equipped with FlowCapt™ acoustic sensors designed to quantify the aeolian snow mass fluxes and to withstand the harsh polar environment. The combination of an AWS and FlowCapt™ sensors is hereafter referred to as an automatic weather and snow station (AWSS). Two generations of FlowCapt™ exist and have been evaluated in the French Alps and in Antarctica (Trouvilliez et al., 2015). Both generations appear to be good detectors of aeolian snow transport events. The first-generation instrument failed to correctly estimate the snow mass flux with the constructor's calibration and even with a new calibration, but the second-generation instrument is capable of providing a lower bound estimate of the snow mass flux and a consistent relationship of the flux versus wind speed.

At each AWSS, FlowCapt™ sensors were set up vertically. When the lower extremity of the sensor is close to the ground or is partially buried, the FlowCapt™ is able to detect the onset of an aeolian snow transport event (i.e., initiation of saltation). Although the level of the snowpack changes over the course of the year due to accumulation and ablation processes, the sensor can nevertheless record continuous observations, which is an advantage over single point measurement devices. The FlowCapt™ has better temporal resolution than visual observations, which are usually made at 6 h intervals. Moreover, the ability of these sensors to detect events of small magnitude is particularly useful, as satellite measurements can only detect blowing snow events in which the snow particles are lifted 20 m or more off the surface in the absence of clouds (Palm et al., 2011). Trouvilliez et al. (2014) reported that aeolian snow transport events with a maximum particle height < 4.5 m above ground level (a.g.l.) accounted for 17 % of the total aeolian snow transport events in the period 2010–2011 at D17 coastal site (Table 1). Ground and satellite observations are thus complementary.

In early 2010, two AWSS equipped with second-generation FlowCapt™ sensors (2G-FlowCapt™) were set up

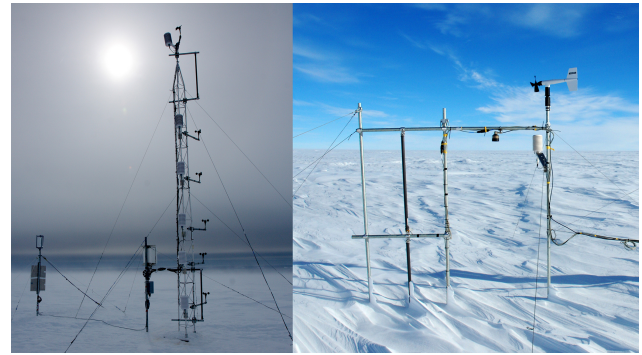


**Figure 2.** Left: the D17 7 m mast with one second-generation FlowCapt™ sensor. Right: the D47 automatic weather and snow station with two second-generation FlowCapt™ sensors.

at sites D17 and D47 (Table 1). Because D47 is located in a dry snow zone roughly 100 km inland from D17, the two stations document distinct climatic conditions. At D17, one 2G-FlowCapt™ was mounted from 0 to 1 m a.g.l. on a 7 m high mast with six levels of cup anemometers and thermo hygrometers, while at D47 a 1 measurement-level AWS was equipped with two 2G-FlowCapt™ installed from 0 to 1 and from 1 to 2 m a.g.l. (Fig. 2). Like the other meteorological variables, the half-hourly mean aeolian snow mass flux recorded by each 2G-FlowCapt™ is stored in the datalogger. An ultrasonic gauge was installed at D47 to monitor surface variations, from which the elevation of sensors above the surface is assessed throughout the year. A detailed description of the equipment at both AWSS can be found in Trouvilliez et al. (2014). Since we focus on the simulated and observed snow mass fluxes, our evaluation is limited to the two stations equipped with 2G-FlowCapt™, i.e., D17 and D47.

### 3 The MAR model

#### 3.1 General description

MAR is a coupled atmosphere/snowpack/aeolian snow transport regional climate model. Atmospheric dynamics is based on the hydrostatic approximation of the primitive equations using the terrain following normalized pressure as a vertical coordinate to account for topography (Gallée and Schayes, 1994). An explicit cloud microphysical scheme describes exchanges between water vapor, cloud droplets, cloud ice crystals (concentration and number), rain drops and snow particles (Gallée, 1995). The original snowpack and aeolian snow transport sub-models are described in Gallée et al. (2001). An improved version is detailed in Gallée et al. (2013) and is used here.

Eroded snow particles drift from the ground into the atmosphere, and the airborne snow particles are advected from one horizontal grid cell to the next one downwind. More generally, airborne snow particles are modeled according to

**Table 1.** Location and characteristics of the two automatic weather and snow stations (AWSS) used in the present study.

	D17	D47
Location	66.7° S, 139.9° E	67.4° S, 138.7° E
Altitude	450 m a.s.l.	1560 m a.s.l.
Distance from coast	10 km	110 km
Period of observation	Since February 2010	January 2010–December 2012
Atmospheric measurements	Wind speed, temperature, and hygrometry at six levels	Wind speed, temperature, and hygrometry at 2 m
Aeolian transport measurements	Second-generation FlowCapt™ from 0 to 1 m	Second-generation FlowCapt™ from 0 to 1 and 1 to 2 m

the microphysical scheme. In particular, the sublimation of windborne snow particles is a function of air relative humidity. Many different types of feedback that are an integral part of aeolian transport of snow are included in MAR. The parameterization of turbulence in the surface boundary layer (SBL) is based on the Monin–Obukhov similarity theory (MO-theory) and accounts for the stabilizing effect of blowing snow particles, as proposed by Wamser and Lykossov (1995). Turbulence above the SBL is parameterized using the local  $E$ – $\varepsilon$  scheme, which consists of two prognostic equations, one for turbulent kinetic energy and the other for its dissipation (Duynkerke, 1988), and includes a parameterization of the turbulent transport of snow particles consistent with classical parameterizations of their sedimentation velocity (Bintanja, 2000). Blowing snow-induced sublimation is computed by the microphysical scheme and influences the heat and moisture budgets in the layers that contain airborne snow particles. Their influence on the radiative transfer through changes in the atmospheric optical depth is taken into account (see Gallée and Gorodetskaya, 2010).

Under near-neutral atmospheric conditions, the MO-theory predicts that the vertical profile of the wind speed within the SBL is semi-logarithmic:

$$u(z) = \frac{u_*}{\kappa} \ln\left(\frac{z}{z_0}\right), \quad (1)$$

where  $u(z)$  is the wind speed at height  $z$ ,  $\kappa = 0.4$  is the von Kármán constant,  $z_0$  is the roughness length for momentum and  $u_*$  is the friction velocity that describes the shear stress exerted by the wind on the surface. Aeolian transport of snow begins when  $u_*$  exceeds the force required for aerodynamic entrainment of snow surface particles, known as threshold friction velocity ( $u_{*t}$ ), which depends on the surface properties of the snow (Gallée et al., 2001). In MAR, surface processes are modeled using the “soil–ice–snow–vegetation–atmosphere transfer” scheme (SISVAT; De Ridder and Gallée, 1998; Gallée et al., 2001; Lefebvre et al., 2005; Fettweis et al., 2005). The threshold friction velocity for a smooth surface ( $u_{*tS}$ ) depends on dendricity, sphericity, and grain size for snow density below  $330 \text{ kg m}^{-3}$  (see Guyomarc’h and Mérindol, 1998), and on snow density alone above  $330 \text{ kg m}^{-3}$ . To account for drag partitioning caused by roughness elements, the threshold friction velocity for a rough surface ( $u_{*tR}$ ) is calculated as in Marticorena and

Bergametti (1995):

$$u_{*tR} = \frac{u_{*tS}}{R_f}, \quad (2)$$

where both threshold friction velocities are expressed in  $\text{m s}^{-1}$  and  $R_f$  is a ratio factor defined as

$$R_f = 1 - \frac{\ln\left(\frac{z_{0R}}{z_{0S}}\right)}{\ln\left[0.35\left(\frac{10}{z_{0S}}\right)^{0.8}\right]}, \quad (3)$$

where  $z_{0R}$  and  $z_{0S}$  are the surface roughness lengths in meters for rough and smooth surfaces, respectively. Over smooth snow surfaces, the roughness length is generally around  $10^{-5}$ – $10^{-4}$  m (Leonard et al., 2011). In MAR, this value is set to  $5 \times 10^{-5}$  m. In addition to the drag partition, moving particles in the saltation layer transfer momentum from the airflow to the surface. Above the saltation layer, the net effect is similar to that of a stationary roughness element (Owen, 1964). Thus, saltation leads to an increase in roughness length compared with a situation without windborne snow, even in the case of a smooth surface. The contribution of blowing snow particles to the roughness length  $z_{0S}$  is calibrated using Byrd project measurements (Budd et al., 1966; Gallée et al., 2001):

$$z_{0S} = 5 \times 10^{-5} + \max\left(0.5 \times 10^{-6}, au_*^2 - b\right), \quad (4)$$

where  $a$  and  $b$  are two constants.

One of the main surface roughness elements in Antarctica is a kind of snow ridge known as sastrugi. These are meter-scale erosional features aligned with the prevailing wind that formed them. The formation of sastrugi may be responsible for an increase in the sastrugi drag coefficient (form drag), leading to an increase in surface roughness and hence to a loss of kinetic energy available for erosion. This is negative feedback for the aeolian transport of snow, as an increase in the roughness length reduces wind speed. Andreas (1995) estimated the timescale for sastrugi formation to be half a day. Sastrugi can be buried if precipitation occurs, thereby reducing surface roughness. All these effects are taken into account in the improved version of the snow-pack sub-model concerning the parameterization of  $z_{0R}$  (see Gallée et al., 2013). Finally, the modeled roughness length results from a combination of  $z_{0S}$  and  $z_{0R}$ . MAR also accounts for the influence of orographic roughness (Jourdain

and Gallée, 2010), but its contribution to the computation of the roughness length was neglected here, as our study is restricted to the coastal slopes of Adélie Land (Fig. 1).

Once aeolian transport begins, the concentration of snow particles in the saltation layer ( $\eta_s$ ), expressed in kilograms of particles per kilograms of air, is parameterized from Pomeroy (1989):

$$\eta_s = \begin{cases} 0 & \text{if } u_{*R} < u_{*tR} \\ e_{\text{salt}} \left( \frac{u_{*R}^2 - u_{*tR}^2}{g h_{\text{salt}}} \right) & \text{if } u_{*R} \geq u_{*tR}, \end{cases} \quad (5)$$

where  $u_{*R}$  is the friction velocity for a rough surface in  $\text{m s}^{-1}$ ,  $e_{\text{salt}}$  is the saltation efficiency equal to 3.25,  $g$  is the gravitational acceleration in  $\text{m s}^{-2}$ , and  $h_{\text{salt}}$  is the saltation height in m, a function of  $u_{*R}$  (Pomeroy and Male, 1992).

As in Gallée et al. (2013), densification of the snowpack by the wind is included in SISVAT from the work of Kotlyakov (1961), i.e., the density of deposited blown snow particles is parameterized as a function of the wind speed at 10 m a.g.l. ( $U_{10}$ ):

$$\rho = 104(U_{10} - 6)^{1/2}, \quad (6)$$

where  $\rho$  is the snow density in  $\text{kg m}^{-3}$  and  $U_{10} > 6 \text{ m s}^{-1}$ . In turn, an increase in the density of the surface snowpack is responsible for an increase in the threshold friction velocity for erosion. This is negative feedback.

### 3.2 Model configuration

MAR was run over Adélie Land for the whole month of January 2011. The modeling grid and setup were the same as those described in Gallée et al. (2013): the integrative domain covers an area of about  $450 \text{ km} \times 450 \text{ km}$  with a 5 km horizontal resolution (Fig. 1). This domain was chosen so as to include the katabatic wind system that develops over the slopes of Adélie Land starting at the break in slope roughly 250 km inland. Since the size of the domain does not significantly influence simulated wind speed (Gallée et al., 2013), we chose a small domain to limit numerical costs. Lateral forcing and sea-surface conditions were taken from ERA-Interim. Sixty vertical levels were used to simulate the atmosphere, with a first level 2 m in height and a vertical resolution of 2 m in the 12 lowest levels. A spin-up, as described in Gallée et al. (2013), was applied so as to achieve relative equilibrium between the snowpack and the atmospheric conditions. The simulation started on 1 December 2010, that is, 1 month before the period in which we were interested.

Erosion of snow by the wind is a highly nonlinear process. Therefore, a good simulation of the atmospheric flow that drives aeolian snow transport events is a prerequisite to simulate the timing of their occurrence for the right reasons. In the model, the roughness length partly depends on wind speed, whose vertical evolution is in turn controlled by the roughness length in a feedback fashion. As in Gallée et

al. (2013),  $z_0$  was calibrated to correctly reproduce the wind minima measured at D17.

### 4 Comparison of field data and model outputs

The aim of this section is to provide a detailed comparison between observed and modeled meteorological variables including aeolian snow mass fluxes. The model performances are assessed using the efficiency statistical test ( $E$ ) proposed by Nash and Sutcliffe (1970):

$$E = 1 - (\text{RMSE}/s)^2, \quad (7)$$

where  $s$  is the standard deviation of the observations and RMSE is the root mean squared error of the simulated variable. An efficiency index of 1 means a perfect simulation (RMSE = 0) and a value of 0 or less means that the model is no better than a minimalist model whose output constantly equals the mean value of the modeled variable over the time period concerned. Wind speed and relative humidity were compared at a height of 2 m above the surface. Simulation data were extracted from the nearest grid point to the AWSS concerned. Simulated snow mass fluxes were first obtained at the coarse resolution (2 m) of the 3-D model. To account for the marked decrease in aeolian snow mass fluxes within the first 2 m, a dimensionless correction factor ( $A$ ) was applied. This factor results from comparing the snow mass fluxes computed in our 3-D MAR simulation and those obtained with a 1-D version of the MAR model using the same parameterization and a higher vertical resolution with five levels describing the first meter above the surface. Corrected snow mass fluxes are calculated as

$$\mu_{1C} = \mu_{1R} A, \quad (8)$$

where  $\mu_{1C}$  is the corrected flux for the lowest layer (0–2 m) and  $\mu_{1R}$  the raw flux from MAR for the lowest layer, both in  $\text{g m}^{-2} \text{ s}^{-1}$ .  $\mu_{1C}$  is compared with the mean observed snow mass flux from 0 to 2 m a.g.l. ( $\mu_{0-2\text{m}}$ ), which is calculated as

$$\mu_{0-2\text{m}} = \frac{\mu_1 h_1 + \mu_2 h_2}{h_1 + h_2}, \quad (9)$$

where  $\mu_i$  is the observed snow mass flux integrated over the emerged length  $h_i$  of the corresponding 2G-FlowCapt™ sensor, in  $\text{g m}^{-2} \text{ s}^{-1}$  and m, respectively.

The comparison first focused on wind speed, which is the driving force behind aeolian snow transport. The timing of aeolian snow transport events was then studied, together with an evaluation of both friction and threshold friction velocities for a period with no concomitant precipitation at site D17. The aeolian snow mass fluxes were then analyzed at D47. We also paid attention to relative humidity so as to evaluate the sublimation of windborne snow particles, since it plays an important role in the ASMB (Lenaerts et al., 2012a). Model sensitivity to roughness length is analyzed in Sect. 4.4.

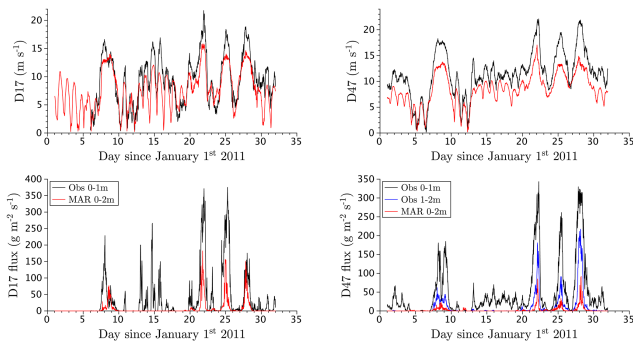


**Figure 3.** Top: observed (black) and simulated (red) wind speed at a height of 2 m. Bottom: aeolian snow transport events: comparison of observed snow mass fluxes from 0 to 1 m (black) and simulated fluxes from 0 to 2 m (red) at the D17 site (bottom left) and at the D47 site (bottom right). Observed snow mass fluxes from 1 to 2 m (blue) are also given for the D47 site.

#### 4.1 Wind speed

Wind speed was correctly simulated by the model (Fig. 3) with an efficiency of 0.60 and 0.37 for D17 and D47, respectively. Variations were correctly represented but wind speeds above  $10 \text{ m s}^{-1}$  were underestimated, particularly at site D47 where the model consistently underestimated wind speed by about  $2 \text{ m s}^{-1}$ . The high efficiency for wind speed at D17 suggests that  $z_0$  might be correctly modeled, while the lower efficiency and the systematic negative bias at D47 strongly suggest overestimation of  $z_0$  at this grid point.

MAR simulated a median  $z_0$  value of 3.2 mm at D17 for our period of interest. This variable could only be compared to observations at D17 since its determination using the profile method (Garrat, 1992) using Eq. (1) requires measurement of wind speed at several levels. During January 2011, atmospheric stratification was mostly near-neutral at D17 owing to mixing caused by katabatic winds. The roughness length  $z_0$  was computed by fitting Eq. (1) with the observed profiles using least-square techniques with the four upper cup anemometers (the two lowest cup anemometers were not functioning correctly). The instruments' elevations above the surface were measured manually at the beginning of January 2011, but variations caused by accumulation/ablation processes during the remainder of the month of January are not known. Errors in measurement heights would introduce a curvature to the modeled wind profile given by Eq. (1) that could produce erroneous values of  $z_0$ . To reduce  $z_0$  uncertainty resulting from this discrepancy, we only considered cases where linear fits were providing determination coefficients above 0.98. This threshold allows removing vertical profiles when wind speed was diverging from logarithmic profiles. The median value of the resulting  $z_0$  was 2.3 mm for the entire month of study, lower but still close to the one simulated by MAR.

This comparison suggests a possible overestimation of  $z_0$  by MAR. Nevertheless, this overestimation is not sufficient to explain the tendency of the model to miss wind maxima. This behavior may also be due to the  $E$ - $\epsilon$  turbulent scheme, which is based on the small eddies concept. During strong winds, turbulent eddies have a large vertical extent and are responsible for the deflection of higher air parcels, which represent a source of momentum that can be transported to the surface in gusts. The  $E$ - $\epsilon$  turbulence scheme cannot reproduce these large eddies or the gusts associated with strong wind events. The use of a non-local turbulence scheme would possibly improve this aspect of the simulation.

Finally, at D47, the original configuration of Gallée et al. (2013) resulted in a median  $z_0$  value of approximately 3.4 mm for the simulated period. Although somewhat higher, this value is consistent with other millimetric  $z_0$  values used in realistic simulations of the Antarctic surface wind field (Reijmer et al., 2004; Lenaerts et al., 2012b). However, the model behaved differently with respect to wind speed depending on the location (Fig. 3). Consequently, a single calibration of  $z_0$  would not represent wind speed with the same accuracy at the two locations.

#### 4.2 Occurrence of aeolian snow transport events

First we compare the observed and simulated aeolian snow transport events in terms of occurrence. The timing of events at D17 and D47 detected by the 2G-FlowCapt<sup>TM</sup> sensor measuring snow particle impacts in the first meter above the surface was correctly simulated by the model except between 12 January and 19 January (Fig. 3). For this period, the field reports mentioned that drifting snow at D17 was limited to less than 1 m above the surface. The same observation was made at D47 as the 2G-FlowCapt<sup>TM</sup> installed from 1 to 2 m above the surface measured negligible snow mass fluxes (Fig. 3). Indeed, MAR failed to reproduce aeolian snow transport events when the maximum particle height was less than 1 m above the surface (Fig. 3). The coarse vertical resolution of the first layers of the MAR (2 m) may explain part of this discrepancy, but corrections of fluxes made with the Eq. (9) should partly account for this aspect. The prevention of erosion in the model may, thus, be related to processes involving snowpack properties and/or friction conditions at the surface. This assumption can be investigated by analyzing both modeled friction and threshold friction velocities.

Like for  $z_0$ , friction and threshold friction velocities were only compared with observations at D17 using the same determination procedure. The 95 % confidence limit of each  $u_*$  was calculated to account for statistical errors associated with the logarithmic profile (Wilkinson, 1984). The lowest 2G-FlowCapt<sup>TM</sup> was in contact with the ground and allowed the detection of aeolian snow transport events:  $u_{*t}$  was computed as the  $u_*$  value as soon as the observed flux value exceeded  $0.001 \text{ g m}^{-2} \text{ s}^{-1}$ . This calculation is only valid without snowfall occurrence. Indeed, when snow falls during

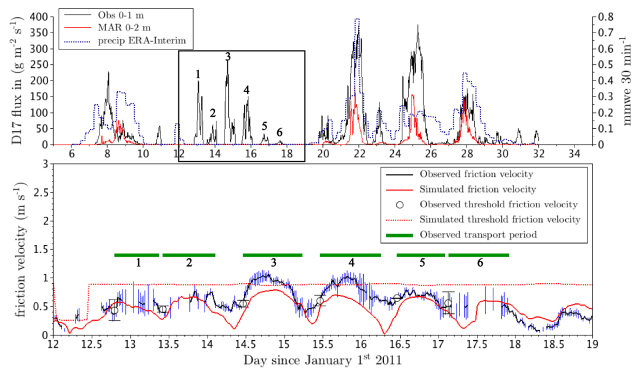


**Figure 4.** Top panel: comparison between observed aeolian snow mass fluxes from 0 to 1 m (black), simulated fluxes from 0 to 2 m (red), and precipitation from ERA-Interim at D17. The black frame identifies the period without precipitation analyzed in the bottom panel. Bottom panel: comparison of observed/simulated friction velocity (black line/red line, respectively) and observed/simulated threshold friction velocity (dashed line/black circles, respectively) at D17 for a transport period with no precipitation. The horizontal green bars represent the observed aeolian snow transport events numbered from 1 to 6.

windy conditions, the sensor detects the presence of airborne snow particles but does not distinguish between precipitating snowflakes and snow grains that were eroded from the surface by the wind. Accounting for situation with snowfall occurrence would introduce a bias in the  $u_{*t}$  values since the detection of an aeolian snow transport event by the 2G-FlowCapt<sup>TM</sup> is not necessarily associated with erosion of snow. Therefore, for an accurate evaluation of  $u_{*t}$ , snowfall events need to be removed from the data. For this purpose, we used the ERA-Interim reanalysis from the European Center for Medium-range Weather Forecast, which appears to be the most appropriate support for estimating precipitation rates in the study area (Palermé et al., 2014). According to the ERA-Interim data, the longest period without precipitation was between 12 January and 19 January. During this period, six transport events were identified and six threshold friction velocities were determined (Fig. 4) from observations. Nevertheless, MAR did not simulate any aeolian snow transport event during the entire period. As shown in Fig. 4, the simulated  $u_*$  is lower than the observed one, while the simulated  $u_{*t}$  is overestimated and higher than the simulated  $u_*$ . This results in the absence of drifting snow in the simulation of this period. Note the decrease in the simulated  $u_{*t}$  in response to the light snowfall that occurred around 12 January (Fig. 4).

Except for cases of drifting snow presented in the previous paragraph, the 2G-FlowCapt<sup>TM</sup> sensors recorded four aeolian snow transport events, which, this time, were simulated by the MAR. Model behavior can be assessed by comparing the relation between aeolian snow mass fluxes versus wind speed for the four strongest events that occurred in

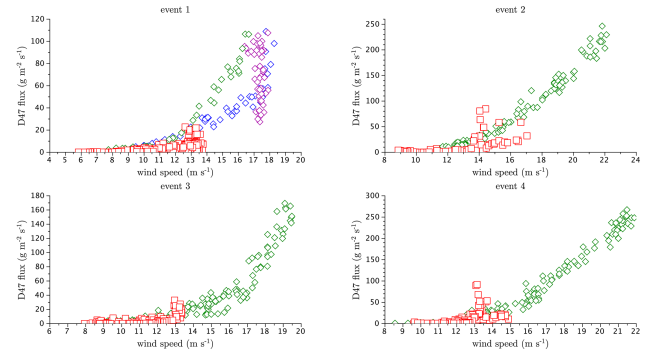


**Figure 5.** Observed (diamonds) and simulated (red squares) snow mass fluxes from 0 to 2 m versus the observed (and simulated respectively) wind speed at 2 m in January 2011 for the four strong aeolian snow transport events recorded at D47. Event 1 lasted from 7–10, event 2 from 21–22, event 3 from 24–26, and event 4 from 27–29 January. For the first event, the observed snow mass fluxes are decomposed in time between a first (blue), an intermediate (purple), and a final relationship (green).

January 2011. It is well known that, at a given height, for a given set of snow particles (i.e., a constant threshold friction velocity value), the amount of snow being transported by the wind can be approximated by a power law of the wind speed (Radok, 1977; Mann et al., 2000). This is clearly depicted in Fig. 5 for events nos. 2, 3, and 4. However, observations show that the occurrence of precipitation may impact this basic relationship, and may explain part of the difference between model and measurements here (see events nos. 2 and 4) (Naaim-Bouvet et al., 2014). Indeed, unlike the others, the first event was characterized by a hysteresis effect (Fig. 5, upper left panel). A similar case was reported by Gordon et al. (2010), who linked this phenomenon to the occurrence of snowfall. This may be justified assuming a 3-stage process of the snow mass flux–wind speed relationship according to changes in  $u_{*t}$  over time: (1) the first stage describes the initiation of the blowing snow event associated with the onset of strong winds: the aeolian snow mass flux increases with wind speed according to the theoretical power law described by Radok (1977), which suggests that  $u_{*t}$  stays roughly unchanged; (2) the second stage is characterized by the relative constancy of the wind speed around  $17\text{--}18 \text{ m s}^{-1}$ , while the aeolian snow mass flux decreases gradually, probably in response to a progressive increase in  $u_{*t}$  (caused by the exhaustion of easily erodible snow or the exposure of a harder layer); (3) finally, ERA-Interim estimates predict the occurrence of substantial precipitation amounts leading the same wind speed to be associated with higher aeolian snow mass fluxes than during the two previous stages; precipitating snow particles and subsequently loosened snow particles are added to the previous set of airborne particles which originate from the surface, and are responsible for a considerable decrease in  $u_{*t}$  below the value estimated in the first stage.

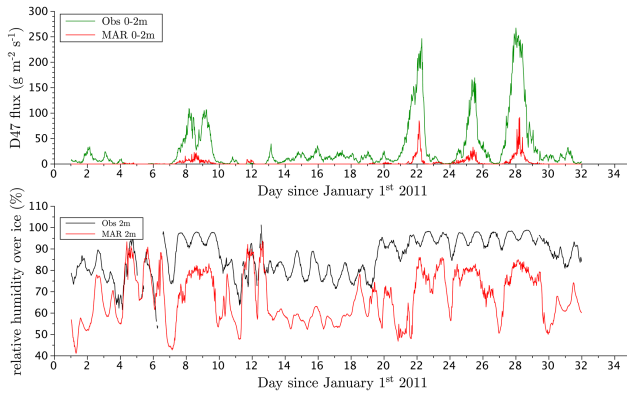


**Figure 6.** Top: observed (green) and simulated (red) snow mass fluxes from 0 to 2 m. Bottom: observed (black) and simulated (red) relative humidity 2 m above the surface.

Then, as the wind weakens, the snow mass flux decreases to negligible values, and the event ends.

Despite the good quality of ERA-Interim precipitation data, we suspect that both modeled occurrences and amounts may differ from observations. The modeled  $u_{*t}$  and horizontal snow transport include biases caused by inaccurately modeled occurrences, which may partly justify that modeled amounts of blowing snow do not exactly fit with a perfect power law of wind speed. Given the previous analysis, the snow mass flux–wind speed relationship is well represented by MAR, suggesting that the model correctly reproduced the underlying processes. The influence of snowfall is also evidenced by the model outputs, showing that the largest simulated snow mass fluxes ( $\sim 90\text{--}100\text{ g m}^{-2}\text{ s}^{-1}$ ) occur at a wind speed of around  $13\text{ m s}^{-1}$ , although the model simulates stronger wind speeds. The second and fourth events (Fig. 5, right panels) are particularly affected. This reflects the decrease in  $u_{*t}$  associated with the heavy snowfall events simulated at that time.

### 4.3 Aeolian snow mass fluxes

Next, we compare the measured aeolian snow mass fluxes and relative humidity with the model outputs in Fig. 6. The evaluation is based only on the AWSS at D47, since this station, unlike D17, provides information on the snow mass fluxes from 0 to 2 m a.g.l., allowing a comparison with the first level of the model. As mentioned above, MAR only simulated aeolian snow transport events at D47 when the maximum particle height was above 1 m. Even in these cases, MAR consistently underestimated the aeolian snow mass fluxes measured by the 2G-FlowCapt<sup>TM</sup>. The modeled underestimation is even higher knowing that the 2G-FlowCapt<sup>TM</sup> sensor already underestimates actual snow mass flux (Trouvilliez et al., 2015). An important negative bias between observed and simulated relative humidity appeared, even when the model correctly simulated the timing of the aeolian snow

**Table 2.** Comparison of Nash tests for wind speed, aeolian snow mass flux, and relative humidity at D47 for various median values of  $z_0$ .

Calibrated $z_0$ (median value, mm)	Wind speed	Snow mass flux	Relative humidity
3	0.37	−0.06	−4.77
0.5	0.8	0.2	−0.14
0.2	0.86	0.26	−0.01
0.1	0.89	0.32	0.16

transport events (Fig. 6). This underestimation may result from the underestimation of the sublimation of the blown snow particles, linked to the underestimation of the concentration of blown snow particles in the lower model layer.

Overall, simulated aeolian snow mass fluxes were twice lower than those provided by the 2G-FlowCapt<sup>TM</sup> sensors for equal wind speed values except during snowfall events. The model also failed to reproduce strong aeolian snow transport events with wind speeds above  $13\text{ m s}^{-1}$  and snow mass fluxes in excess of  $100\text{ g m}^{-2}\text{ s}^{-1}$ . As a result, the simulated horizontal snow transport through the first 2 m a.g.l. at D47 in January 2011 was underestimated by roughly a factor of 10 compared to observations; the model calculated  $5768\text{ kg m}^{-2}$ , while the 2G-FlowCapt<sup>TM</sup> measured  $67\,509\text{ kg m}^{-2}$ .

### 4.4 Model sensitivity to roughness length for momentum

Since wind speed is the most important force behind snow erosion (Gallée et al., 2013), we performed a sensitivity test to see whether lower  $z_0$  was giving more accurate modeled wind speed values. We tuned the model with different  $z_0$  values to assess wind speed relationship with  $z_0$ . According to theory, the higher the wind speed, the higher the snow mass fluxes. As a consequence, larger relative humidity was modeled close to the surface with lower  $z_0$ . This resulted from sublimation of additional windborne snow particles in the lowest levels of the model. The model evaluation was performed with wind speed values measured at D47 over the entire study period. Results for various median  $z_0$  values are summarized in Table 2. The best results were obtained for a reduction of  $z_0$  by a factor of 30 (i.e., a median  $z_0$  value of 0.1 mm) over the simulated period at D47. The corresponding statistical efficiency for wind speed reached 0.89, while the efficiencies of the snow mass flux and relative humidity both became positive. The resulting local snow transport was still underestimated but only by about one third of the observed value. Nevertheless, reducing  $z_0$  did not enable the reproduction of the small drifting snow events that occurred between 12 January and 19 January, suggesting that part of the processes leading to surface state evolution is not fully re-



produced by the MAR. Therefore, further improvements are still necessary.

## 5 Discussion

The original calibration of  $z_0$  (Gallée et al., 2013) produced satisfactory results for modeled wind speed at D17, but the same good behavior was not reproduced at D47, another measurement point located 100 km away. We showed that a 1-order decrease in the magnitude of  $z_0$  significantly improved the simulation quality at D47, but we cannot affirm that this modification gives a more relevant  $z_0$  for this site. In other words, obtaining a better representation of the evaluated variables does not mean that modeled  $z_0$  agreed with observed  $z_0$  or that the processes governing its behavior were correctly modeled. This may be the result of error compensations.

Nevertheless, this suggests that  $z_0$  may vary regionally. In particular, D17 and D47 are located on either side of the dry-snow line, and the temperature regime at the two locations is sufficiently contrasted to explain differences in snowpack properties such as internal cohesion, density or aerodynamic resistance, which are involved in different types of feedback between  $z_0$  and snow transport by the wind. In this case, distributed modeling should account for spatial variations of  $z_0$  to allow a consistent representation of the aeolian snow mass fluxes. Smeets and van den Broeke (2008) showed that  $z_0$  can vary from 2 to 3 orders of magnitude during the ablation season between coastal and inland locations situated on either side of the equilibrium line of West Greenland. Consequences on wind speed and aeolian snow mass fluxes would be important, as demonstrated at D17, where the agreement between modeled and observed wind speed was significantly reduced assuming a lower  $z_0$  value. Indeed, the modeled wind speed bias increased from  $-1$  to  $+1.5 \text{ m s}^{-1}$  for the entire simulated period when  $z_0$  was changed from 3.2 to 0.1 mm. Further investigations of  $z_0$  and its linkages with snow transport by the wind in Adélie Land are thus required.

Using the original calibration, the simulated horizontal snow transport in the first 2 m above the surface at site D47 in January 2011 was about 10 times lower than the observed value. This difference could mainly be explained by overestimation of the modeled  $z_0$  and subsequent underestimation of the wind speed. The drag partition dictating the form drag in the MAR is currently parameterized with a qualitative formulation (Gallée et al., 2013) adapted from the work of Andreas and Claffey (1995) on sea ice in the Weddell Sea. Validity of this formulation should be reassessed given the differences in surface drag properties between coastal margins of Adélie Land and sea ice. Indeed, the severe katabatic wind regime characterizing the slopes of Adélie Land may promote aerodynamical adjustment of the snow surface. Thus, the form drag is likely lower than for sea ice, which experiences much lower wind speeds. In particular, overestimation of  $z_0$  in the

simulation resulted in a deficit of shear stress available for snow erosion, thus leading to underestimation of the modeled snow mass fluxes. As form drag is the main contributor to surface transfer of momentum (Jackson and Carroll, 1978; Andreas, 1995; Smeets and van den Broeke, 2008) over rough snow/ice fields, a more sophisticated representation of  $z_0$  that accounts for potential spatial and temporal variations in the form drag in the model is needed.

## 6 Conclusions

The regional climate model MAR, which includes a coupled snowpack/aeolian snow transport parameterization, was run at a fine spatial resolution (5 km horizontally and 2 m vertically) for a period of 1 summer month in coastal Adélie Land, East Antarctica. The study reported here is a step forward in the model evaluation of the aeolian transport of snow. The study by Gallée et al. (2013) focused on checking that the MAR was able to reproduce drifting snow occurrences in January 2010 at one near-coastline location (D3,  $\sim 5$  km from the coast) in Adélie Land. In this paper, using the same model setup, we present a quantitative evaluation of the aeolian erosion process in the same region, by comparing model outputs with (1) observed aeolian snow mass fluxes and relative humidity at D47 ( $\sim 100$  km from the coast) in January 2011, and (2) observed friction velocity and threshold friction velocity for snow transport over a 7-day period without precipitation in January 2011 at D17 (located  $\sim 10$  km from the coast). This comparison highlighted the model qualities and discrepancies. Firstly, wind speed variations were accurately represented by the MAR although the model underestimated the wind maxima at D17 and more generally the wind speed at D47. This underestimation may be justified by an incomplete representation of  $z_0$  and by the use of a turbulent scheme based on the small eddies concept. Secondly, the occurrence of the aeolian snow transport events was well reproduced except for events when the maximum particle height was less than 1 m above the surface. This probably results from a combination of underestimation of the friction velocity, overestimation of the threshold friction velocity and the too-coarse vertical resolution (2 m) of the MAR near the surface. Thirdly, at the same wind speed, modeled snow mass fluxes were twice lower than those measured by the 2G-FlowCapt™ sensor, while it is known that this sensor already underestimates the snow mass fluxes of aeolian snow transport. Finally, the model underestimated the large snow mass fluxes ( $> 100 \text{ g m}^{-2} \text{ s}^{-1}$ ) and the associated strong winds ( $> 13 \text{ m s}^{-1}$ ). Comparison with measurements from 2G-FlowCapt™ sensors at D47 revealed that the model underestimates the horizontal snow transport over the first 2 m above the ground by a factor of 10. Our results show that using the original setup of Gallée et al. (2013), MAR would significantly underestimate the contribution of aeolian snow transport to the ASMB. For that reason, new observations

are currently underway to better assess the contribution of the form drag to  $z_0$  in coastal Adélie Land and to develop a more robust calibration process for  $z_0$ .

*Acknowledgements.* This comparison would not have been possible without the financial support of the European program FP-7 ICE2SEA, grant no. 226375, and the financial and logistical support of the French Polar Institute IPEV (program CALVA-1013). Additional support by INSU through the LEFE/CLAPA project and OSUG through the CENACLAM/GLACIOCLIM observatory is also acknowledged. The MAR simulations were run on CNRS/IDRIS and Université Joseph Fourier CIMENT computers. We would like to thank all the on-site personnel in Dumont d'Urville and Cap Prud'homme for providing precious help in the field, and the two anonymous reviewers for their constructive remarks that helped to improve the manuscript considerably.

Edited by: P. Marsh

## References

- Agosta, C., Favier, V., Genthon, C., Gallée, H., Krinner, G., Lenaerts, J. T. M., and van den Broeke, M. R.: A 40-year accumulation dataset for Adélie Land, Antarctica and its application for model validation, *Clim. Dynam.*, 38, 75–86, doi:10.1007/s00382-011-1103-4, 2012.
- Andreas, E. L.: Air-ice drag coefficients in the western Weddell sea. 2. A model based on form drag and drifting snow, *J. Geophys. Res.*, 100, 4833–4843, 1995.
- Andreas, E. L. and Claffey, K. J.: Air-ice drag coefficients in the western Weddell sea. 1. Values deduced from profile measurements, *J. Geophys. Res.*, 100, 4821–4831, 1995.
- Bintanja, R.: Snowdrift suspension and atmospheric turbulence. Part I: Theoretical background and model description, *Bound.-Layer Meteorol.*, 95, 343–368, 2000.
- Budd, W. F.: The drifting of nonuniform snow particles, in: *Studies in Antarctic Meteorology*, Vol. 9, 59–70, AGU, Washington DC, 1966.
- Budd, W. F., Dingle, W. R. J., and Radok, U.: The Byrd snow drift project outline and basic results, in: *Studies in Antarctic Meteorology*, Vol. 9, edited by: Rubin, M. J., 71–134, American Geophysical Union, Washington DC, 1966.
- Cierco, F.-X., Naaim-Bouvet, F., and Bellot, H.: Acoustic sensors for snowdrift measurements: How should they be used for research purposes?, *Cold Reg. Sci. Technol.*, 49, 74–87, doi:10.1016/j.coldregions.2007.01.002, 2007.
- Das, I., Bell, R. E., Scambos, T. A., Wolovick, M., Creyts, T. T., Studinger, M., Frearson, N., Nicolas, J. P., Lenaerts, J. T. M., and van den Broeke, M. R.: Influence of persistent wind scour on the surface mass balance of Antarctica, *Nat. Geosci.*, 6, 367–371, 2013.
- De Ridder, K. and Gallée, H.: Land Surface-Induced Regional Climate Change in Southern Israel, *J. Appl. Meteorol.*, 37, 1470–1485, doi:10.1175/1520-0450(1998)037<1470:LSIRCC>2.0.CO;2, 1998.
- Déry, S. J. and Yau, M. K.: Large-scale mass balance effects of blowing snow and surface sublimation, *J. Geophys. Res.*, 107, 4679, doi:10.1029/2001JD001251, 2002.
- Duynkerke, P. G.: Application of the  $E - \epsilon$  Turbulence Closure Model to the Neutral and Stable Atmospheric Boundary Layer, *J. Atmos. Sci.*, 45, 865–880, 1988.
- Favier, V., Agosta, C., Genthon, C., Arnaud, L., Trouvillez, A., and Gallée, H.: Modeling the mass and surface heat budgets in a coastal blue ice area of Adélie Land, Antarctica, *J. Geophys. Res.*, 116, F03017, doi:10.1029/2010JF001939, 2011.
- Fettweis, X., Gallée, H., Lefebvre, F., and Van Ypersele, J.: Greenland Surface Mass Balance simulated by a Regional Climate Model and Comparison with satellite derived data in 1990–1991, *Clim. Dynam.*, 24, 623–640, doi:10.1007/s00382-005-0010-y, 2005.
- Frezzotti, M., Gandolfi, S., and Urbini, S.: Snow megadunes in Antarctica: Sedimentary structure and genesis, *J. Geophys. Res.*, 107, 4344, doi:10.1029/2001JD000673, 2002.
- Frezzotti, M., Pourchet, M., Flora, O., Gandolfi, S., Gay, M., Urbini, S., Vincent, C., Becagli, S., Gragnani, R., Proposito, M., Severi, M. T. R., Udisti, R., and Fily, M.: New Estimations of Precipitation and Surface Sublimation in East Antarctica from Snow Accumulation Measurements, *Clim. Dynam.*, 23, 803–813, 2004.
- Gallée, H.: Simulation of the Mesocyclonic Activity in the Ross Sea, Antarctica, *Mon. Weather Rev.*, 123, 2051–2069, 1995.
- Gallée, H.: A simulation of blowing snow over the Antarctic ice sheet, *Ann. Glaciol.*, 26, 203–205, 1998.
- Gallée, H. and Gorodetskaya, I. V.: Validation of a limited area model over Dome C, Antarctic Plateau, during winter, *Clim. Dynam.*, 34, 61–72, doi:10.1007/s00382-008-0499-y, 2010.
- Gallée, H. and Schayes, G.: Development of a three-dimensional meso- $\gamma$  primitive equation model: katabatic winds simulation in the area of Terra Nova Bay, Antarctica, *Mon. Weather Rev.*, 122, 671–685, 1994.
- Gallée, H., Guyomarc'h, G., and Brun, É.: Impact of snow drift on the antarctic ice sheet surface mass balance: possible sensitivity to snow-surface properties, *Bound.-Layer Meteorol.*, 99, 1–19, 2001.
- Gallée, H., Peyaud, V., and Goodwin, I.: Simulation of the net snow accumulation along the Wilkes Land transect, Antarctica, with a regional climate model, *Ann. Glaciol.*, 41(January), 1–6, 2005.
- Gallée, H., Trouvillez, A., Agosta, C., Genthon, C., Favier, V., and Naaim-Bouvet, F.: Transport of Snow by the Wind: A Comparison Between Observations in Adélie Land, Antarctica, and Simulations Made with the Regional Climate Model MAR, *Bound.-Layer Meteorol.*, 146, 133–147, doi:10.1007/s10546-012-9764-z, 2013.
- Garcia, R.: Mesures de transport de neige par le vent à la station Charcot, *La météorologie*, 57, 205–213, 1960.
- Garratt, J. R.: *The Atmospheric Boundary Layer*, Cambridge University Press, Cambridge, 1992.
- Genthon, C., Lardeux, P., and Krinner, G.: The surface accumulation and ablation of a coastal blue-ice area near Cap Prudhomme, Terre Adélie, Antarctica, *J. Glaciol.*, 53, 635–645, 2007.
- Gordon, M., Biswas, S., Taylor, P. A., Hanesiak, J., Albarran-Melzer, M., and Fargey, S.: Measurements of drifting and blowing snow at Iqaluit, Nunavut, Canada during the star project, *Atmos.-Ocean*, 48, 81–100, doi:10.3137/AO1105.2010, 2010.
- Guyomarc'h, G. and Méridol, L.: Validation of an application for forecasting blowing snow, *Ann. Glaciol.*, 26, 138–143, 1998.

- Jackson, B. S. and Carroll, J. J.: Aerodynamic roughness as a function of wind direction over asymmetric surface elements, *Bound.-Layer Meteorol.*, 14, 323–330, 1978.
- Jourdain, N. C. and Gallée, H.: Influence of the orographic roughness of glacier valleys across the Transantarctic Mountains in an atmospheric regional model, *Clim. Dynam.*, 36, 1067–1081, doi:10.1007/s00382-010-0757-7, 2010.
- Kodama, Y., Wendler, G., and Gosink, J.: The effect of blowing snow on katabatic winds in Antarctica, *Ann. Glaciol.*, 6, 59–62, 1985.
- Kotlyakov, V. M.: Results of a Study of the Processes of Formation and Structure of the Upper Layer of the Ice Sheet in Eastern Antarctica, in: *Symposium on Antarctic Glaciology*, 88–99, IAHS Publication, Helsinki, 1961.
- Lefebvre, F., Fettweis, X., Gallée, H., Van Ypersele, J., Marbaix, P., Greuell, W., and Calanca, P.: Evaluation of a high-resolution regional climate simulation over Greenland, *Clim. Dynam.*, 25, 99–116, doi:10.1007/s00382-005-0005-8, 2005.
- Lenaerts, J. T. M., van den Broeke, M. R., Déry, S. J., König-Langlo, G., Ettema, J., and Munneke, P. K.: Modelling snowdrift sublimation on an Antarctic ice shelf, *The Cryosphere*, 4, 179–190, doi:10.5194/tc-4-179-2010, 2010.
- Lenaerts, J. T. M., van den Broeke, M. R., van de Berg, W. J., van Meijgaard, E., and Kuipers Munneke, P.: A new, high-resolution surface mass balance map of Antarctica (1979–2010) based on regional atmospheric climate modeling, *Geophys. Res. Lett.*, 39, L0451, doi:10.1029/2011GL050713, 2012a.
- Lenaerts, J. T. M., van den Broeke, M. R., Déry, S. J., van Meijgaard, E., van de Berg, W. J., Palm, S. P., and Sanz Rodrigo, J.: Modeling drifting snow in Antarctica with a regional climate model: 1. Methods and model evaluation, *J. Geophys. Res.*, 117, D05108, doi:10.1029/2011JD016145, 2012b.
- Lenaerts, J. T. M., van den Broeke, M. R., Scarchilli, C., and Agosta, C.: Impact of model resolution on simulated wind, drifting snow and surface mass balance in Terre Adélie, East Antarctica, *J. Glaciol.*, 58, 821–829, doi:10.3189/2012JoG12J020, 2012c.
- Leonard, K. C., Tremblay, L.-B., Thom, J. E., and MacAyeal, D. R.: Drifting snow threshold measurements near McMurdo station, Antarctica: A sensor comparison study, *Cold Reg. Sci. Technol.*, 70, 71–80, doi:10.1016/j.coldregions.2011.08.001, 2011.
- Lorius, C.: Contribution to the knowledge of the Antarctic ice sheet: a synthesis of glaciological measurements in Terre Adélie, *J. Glaciol.*, 4, 79–92, 1962.
- Madigan, C. T.: Meteorology. Tabulated and reduced records of the Cape Denison Station, Adélie Land. Australasian Antarctic Expedition 1911–1914 Scientific Reports, Serie B, Vol. 4, 1929.
- Mann, G. W., Anderson, P. S., and Mobbs, S. D.: Profile measurements of blowing snow at Halley, Antarctica, *J. Geophys. Res.*, 105, 24491–24508, doi:10.1029/2000JD900247, 2000.
- Martcorena, B. and Bergametti, G.: Modeling the atmospheric dust cycle: 1. Design of a soil-derived dust emission scheme, *J. Geophys. Res.*, 100, 16415–16430, 1995.
- Naaim-Bouvet, F., Bellot, H., and Naaim, M.: Back analysis of drifting-snow measurements over an instrumented mountainous site, *Ann. Glaciol.*, 51, 207–217, doi:10.3189/172756410791386661, 2010.
- Naaim-Bouvet, F., Bellot, H., Nishimura, K., Genthon, C., Palerme C., Guyomarc’h, G., and Vionnet, V.: Detection of snow-fall occurrence during blowing snow events using photo-electric sensors, *Cold Reg. Sci. Technol.*, 106–107, 11–21, doi:10.1016/j.coldregions.2014.05.005, 2014.
- Nash, J. E. and Sutcliffe, J. V.: River flow forecasting through conceptual models Part I – A discussion of principles, *J. Hydrol.*, 10, 282–290, 1970.
- Owen, P. R.: Saltation of uniform grains in air, *J. Fluid Mech.*, 20, 225–242, 1964.
- Palerme, C., Kay, J. E., Genthon, C., L’Ecuyer, T., Wood, N. B., and Claud, C.: How much snow falls on the Antarctic ice sheet?, *The Cryosphere*, 8, 1577–1587, doi:10.5194/tc-8-1577-2014, 2014.
- Palm, S. P., Yang, Y., Spinhirne, J. D., and Marshak, A.: Satellite remote sensing of blowing snow properties over Antarctica, *J. Geophys. Res.*, 116, D16123, doi:10.1029/2011JD015828, 2011.
- Parish, T. R. and Wendler, G.: The katabatic wind regime at Adélie Land, Antarctica, *Int. J. Climatol.*, 11, 97–107, 1991.
- Pomeroy, J. W.: A process-based model of snow drifting, *J. Glaciol.*, 13, 237–240, 1989.
- Pomeroy, J. W. and Male, D. H.: Steady-state suspension of snow, *J. Hydrol.*, 136, 275–301, doi:10.1016/0022-1694(92)90015-N, 1992.
- Prud’homme, A. and Valtat, B.: Les observations météorologiques en Terre Adélie 1950–1952 – Analyse critique, *Expéditions polaires françaises*, Paris, 1957.
- Radok, U.: Snow Drift, *J. Glaciol.*, 19, 123–139, 1977.
- Reijmer, C. H., van Meijgaard, E., and van den Broeke, M. R.: Numerical studies with a regional atmospheric climate model based on changes in the roughness length for momentum and heat over Antarctica, *Bound.-Layer Meteorol.*, 111, 313–337, 2004.
- Scarchilli, C., Frezzotti, M., Grigioni, P., De Silvestri, L., Agnoletto, L., and Dolci, S.: Extraordinary blowing snow transport events in East Antarctica, *Clim. Dynam.*, 34, 1195–1206, doi:10.1007/s00382-009-0601-0, 2010.
- Smeets, C. J. P. P. and van den Broeke, M. R.: Temporal and spatial variations of the aerodynamic roughness length in the ablation zone of the Greenland Ice Sheet, *Bound.-Layer Meteorol.*, 128, 315–338, 2008.
- Trouvilliez, A., Naaim-Bouvet, F., Genthon, C., Piard, L., Favier, V., Bellot, H., Agosta, C., Palerme, C., Amory, C., and Gallée, H.: A novel experimental study of aeolian snow transport in Adélie Land (Antarctica), *Cold Reg. Sci. Technol.*, 108, 125–138, doi:10.1016/j.coldregions.2014.09.005, 2014.
- Trouvilliez, A., Naaim-Bouvet, F., Bellot, H., Genthon, C., and Gallée, H.: Evaluation of Flowcapt acoustic sensor for snowdrift measurements, *J. Atmos. Ocean. Tech.*, in press, 2015.
- Wamser, C. and Lykossov, V. N.: On the friction velocity during blowing snow, *Contrib. to Atmos. Phys.*, 68, 85–94, 1995.
- Wendler, G.: On the blowing snow in Adélie Land, eastern Antarctica. A contribution to I.A.G.O., in: *Glacier fluctuations and climatic change*, edited by: Oerlemans, J., 261–279, Reidel, Dordrecht, 1989.
- Wendler, G., Stearns, C. R., Dargaud, G., and Parish, T. R.: On the extraordinary katabatic winds of Adélie Land, *J. Geophys. Res.*, 102, 4463–4474, 1997.
- Wilkinson, R. H.: A Method for Evaluating Statistical Errors Associated with Logarithmic Velocity Profiles, *Geo-Marine Lett.*, 3, 49–52, 1984.
- Xiao, J., Bintanja, R., Déry, S. J., Mann, G. W., and Taylor, P. A.: An intercomparison among four models of blowing snow, *Bound. Layer Meteorol.*, 97, 109–135, 2000.